ELSEVIER

Journal of Nuclear Materials 290–293 (2001) 107–111

journal of nuclear materials

www.elsevier.nl/locate/jnucmat

Synergistic effects by simultaneous bombardment of tungsten with hydrogen and carbon

K. Krieger *, J. Roth

Max-Plank-Institut für Plasmaphysik, IPP-EURATOM Association, Boltzmannstraße 2, Garching 85746 , Germany

Abstract

The simultaneous bombardment of a W surface by hydrogen isotopes and carbon impurities leads to synergistic effects with significantly different plasma–wall interaction properties compared to the ones of pure hydrogen or pure carbon bombardment. Simultaneous impact of carbon and hydrogen ions has been realised by irradiation of W targets with CH_3^+ radicals produced by a high current ion source. For comparison, the same experiment was also carried out with C^+ ions. The measured evolution of the target weight as a function of irradiation fluence and the final amount of deposited carbon are compared to a simple model of erosion–deposition balance. This allows one to derive the dependence of the carbon sputtering yield on both the impacting ion species and the target temperature.

Keywords: Erosion; Tungsten; Carbon; First wall materials

1. Introduction

For plasma-facing components of future fusion devices it will likely be necessary to use several different materials. This is because there is, at present, no known material, which can meet the necessary physical and technical requirements at all first wall and divertor locations. A promising material combination in divertor machines is carbon for the strike point zones of the target plates, which alleviates the effect of potential power excursions, and tungsten for the baffle region at the divertor throat. Outside the divertor, carbon-based materials might also be used as material for start-up limiters. In such a configuration carbon will migrate through the plasma and redeposit also at the tungsten surfaces [1]. The simultaneous bombardment of the W surface by hydrogen isotopes and carbon impurities leads to synergistic effects with significantly different plasma–wall interaction properties compared to the ones of pure hydrogen or pure carbon bombardment.

To study the underlying physical processes under controlled conditions, the simultaneous impact of carbon and hydrogen ions has been realised by irradiation of a W target with CH_3^+ radicals produced by an ion source. For comparison, the same experiment was also carried out using C^+ ions. Earlier investigations have shown that the experimental data for C^+ impact on tungsten at room temperature are well reproduced by TRIDYN simulations [2]. The simulations failed, however, to reproduce the experimental results for C^+ impact at elevated target temperatures as well as the results for CH_3^+ impact. There have been attempts to explain the results for C^+ impact at elevated temperatures by including diffusion effects into the simulation [3]. It is obvious, nevertheless, that the models for the basic physical processes in the simulations are incomplete. In this paper, therefore, a simple phenomenological model is introduced to describe the particle balance between erosion and deposition on the target by a set of material parameters such as erosion yields and reflection coefficients. The model is compared to the experimental data and used to obtain information on the interdependencies of the included parameters.

* Corresponding author. Tel.: +49-89 32 99 1655; fax: +49-89 32 99 2279.

E-mail address: krieger@ipp.mpg.de (K. Krieger).

0022-3115/01/$ - see front matter
PII: S0022-3115(00)00611-5

2. Experimental

Tungsten targets with temperatures ranging from room temperature up to 800°C were irradiated with CH_3^+ radicals and C^+ ions, respectively. The energies of the radical ion beam (3 keV) and of the pure carbon ion beam (2.4 keV) were chosen such that the energy of the impacting carbon atoms was always the same [2]. During the bombardment process, the weight change of the tungsten samples was determined at different fluences using an in situ microbalance with an accuracy of better than 1 μg. At the end of the irradiation procedure the amount of carbon in the surface layer of the samples was determined simultaneously by nuclear reaction analysis (NRA) using the reaction $^{12}C(^3He, p_1)^{14}N$ and by Rutherford back-scattering analysis (RBS) [2].

3. Model

Similar to the ansatz by Naujoks et al. [4,5] we describe the erosion of target material and the implantation and re-erosion of impacting ions by a set of rate differential equations:

$$\frac{dn_C}{dt} = \Gamma_C(1-(1-f_C)R) - \Gamma_C f_C \underbrace{\left(Y_C^C + \frac{\Gamma_H}{\Gamma_C} Y_C^H\right)}_{Y_C}, \qquad (1)$$

$$\frac{dn_W}{dt} = -\Gamma_C(1-f_C)Y_W^C,$$

where n_C and n_W are the eroded/implanted fluences of carbon and tungsten from/to the target. Γ_C and Γ_H denote, respectively, the carbon and hydrogen flux impacting at the target. R is the reflection coefficient of the carbon ions at the pure tungsten surface and Y_x^y is the sputtering yield of element x bombarded by element y. With increasing carbon concentration the reflection coefficient decreases to approximately zero for a pure carbon surface. This is taken into account by multiplying R by $1-f_C$. Further, we assume that erosion and deposition processes occur uniformly distributed in a layer of constant thickness and density with, correspondingly, constant area density $\tilde{n} = \tilde{n}_C + \tilde{n}_W$ of carbon and tungsten atoms. $f_C = \tilde{n}_C/\tilde{n}$ represents the carbon concentration at the target surface, which is assumed to be constant in the layer. $\tilde{n}$ does not correspond to the actual penetration depth of the impacting ions, which is much smaller than the thickness of the model layer. Within the frame of the model $\tilde{n}$ in fact represents the typical fluence scale of the system to reach stationary conditions.

Since the thickness of the layer is a constant, the addition or removal of particles at the surface must be balanced by a corresponding particle source or sink at the interface to the target bulk material. In case of net deposition, $dn_C/dt + dn_W/dt > 0$, we define a sink weighted with the concentration of the respective species:

$$\frac{d\tilde{n}_C}{dt} = \frac{dn_C}{dt} - f_C\left(\frac{dn_C}{dt} + \frac{dn_W}{dt}\right). \qquad (2)$$

Using this relation one obtains a non-linear differential equation for $f_C(t)$:

$$\begin{aligned}\frac{df_C}{dt} &= \frac{1}{\tilde{n}}\frac{d\tilde{n}_C}{dt} \\ &= \frac{\Gamma_C}{\tilde{n}}\left((1-R) + \left(1-2R+Y_C-Y_W^C\right)f_C - \left(Y_C - Y_W^C - R\right)f_C^2\right). \end{aligned} \qquad (3)$$

One can solve the equation analytically and obtain:

$$\begin{aligned} f_C &\overset{Y_C - Y_W^C \neq 1}{=} \frac{1-\exp\left(\left(1-Y_C+Y_W^C\right)(\Gamma_C t/\tilde{n})\right)}{\frac{Y_C-Y_W^C-R}{1-R} - \exp\left(\left(1-Y_C+Y_W^C\right)(\Gamma_C t/\tilde{n})\right)}, \\ f_C &\overset{Y_C - Y_W^C = 1}{=} \frac{(1-R)\Gamma_C t}{\tilde{n} + (1-R)\Gamma_C t}. \end{aligned} \qquad (4)$$

In case of net erosion, the corresponding particle source consists only of tungsten and therefore

$$\frac{d\tilde{n}_C}{dt} = \frac{dn_C}{dt}. \qquad (5)$$

This leads to a linear differential equation for $f_C(t)$:

$$\frac{df_C}{dt} = \frac{\Gamma_C}{\tilde{n}}(1-R-(Y_C-R)f_C) \qquad (6)$$

with the solution

$$f_C = \frac{1-R}{Y_C-R}\left(1-\exp\left(-(Y_C-R)\frac{\Gamma_C t}{\tilde{n}}\right)\right). \qquad (7)$$

Fig. 1 shows the solutions for the two cases of net erosion and net deposition. It should be noted that cases of initial net deposition can turn into net erosion at a certain fluence and vice versa.

Inserting Eqs. (4) and (7) in (1), one can solve for $n_C(t)$ and $n_W(t)$. The weight change of the target is then given by

$$\Delta w = m_C n_C + m_W n_W, \qquad (8)$$

which can be compared with the measured evolution of the weight change as a function of fluence. Furthermore, the total amount of carbon measured after irradiation corresponds to $n_C(t_{end})$.

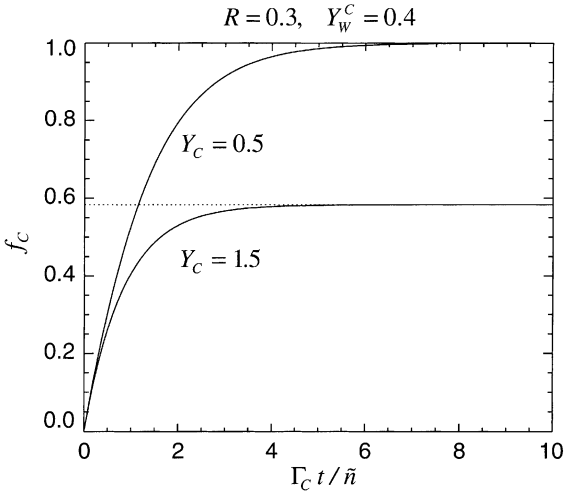

Fig. 1. Time evolution of f_C for a case with net deposition ($Y_C = 0.5$) and net erosion ($Y_C = 1.5$).

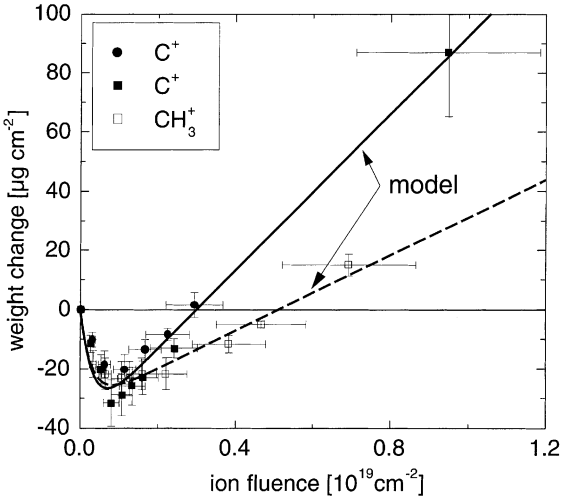

Fig. 2. Weight change of tungsten targets at room temperature as a function of irradiation fluence. For C^+, the experiments were performed on two targets denoted by circles and squares. In addition, the graph shows the weight change according to the analytical model with parameters fitted to the experimental results.

4. Results and discussion

4.1. Weight change measurements

A set of targets was irradiated, with both C^+ and CH_3^+ species, at different temperatures, ranging from room temperature up to 800°C. The particle energy was 2.4 keV for C^+ and 3 keV for CH_3^+ . In the case of CH_3^+, it is assumed that the energy is distributed according to the atomic masses upon fragmentation in the target [2]. The resulting energy of the carbon ions is therefore the same in both cases.

Fig. 2 shows the weight change as a function of fluence for CH_3^+ and C^+ irradiation of targets at room temperature. In both cases the probe initially loses weight due to erosion of tungsten. Because of the enrichment of carbon in the surface layer, the erosion decreases until, at a certain fluence, the weight gain due to deposition of carbon prevails. In the case of CH_3^+, the maximum weight loss and the slope of the weight increase after reaching equilibrium conditions is smaller than in the case of C^+.

The weight loss according to the model described in Section 2 (Eq. (8)) was fitted to the experimental data by assuming a tungsten reflection coefficient of $R = 0.39$ [6], and a tungsten sputtering yield, for carbon impact, of $Y_W^C = 0.37$ according to TRIM simulations [7]. The carbon erosion rate, Y_C, and the scaling fluence, $\tilde{n}$, were used as fit parameters. As can be seen in Fig. 2, there is a very good agreement between the model and the experimental results. The resulting fit parameters are $Y_C = 0.34$, $\tilde{n} = 2.8 \times 10^{17}$ cm^{-2} for C^+ irradiation. For CH_3^+ irradiation one obtains $Y_C = 0.68$, $\tilde{n} = 2 \times 10^{17}$ cm^{-2}. The increase of the carbon erosion yield due to the additional impact of hydrogen, taking also into account chemical erosion, is $Y_C^H \Gamma_H / \Gamma_C = 3 Y_C^H \approx 0.03$ [7]. This value is too small to account for the experimental difference between the C^+ and CH_3^+ behaviour as an effect of a linear superposition of carbon self-sputtering and erosion by hydrogen. One might assume that the additional dilution of the near-surface area by implanted hydrogen, which is not included in the model discussed above, might lead to a slower growth of the carbon deposition. TRIDYN simulations have shown that the resulting effect is also much smaller than necessary to explain the observations [2].

The weight change for irradiation of targets at 500°C is shown in Fig. 3. At this temperature, the weight change, as a function of irradiation fluence for C^+ bombardment, shows a similar behaviour as for room temperature. The slope of the weight gain due to carbon deposition is, however, significantly smaller. For CH_3^+ bombardment one finds a completely different behaviour. The weight loss as a function of irradiation fluence is much steeper and there is no sign of a turn-over to deposition within the range of fluences covered by the experiment. This is also reflected by the parameters obtained in fitting the modelled weight loss to the experimental data, where the erosion yield for the CH_3^+ bombardment, $Y_C = 1.61$, now exceeds 1. For C^+ the respective value is $Y_C = 0.67$. It should be noted, however, that experimental uncertainties, in the case of net erosion, are considerably larger because the experimental data cover only a limited fluence range. A minimum with subsequent net deposition at even higher fluences,

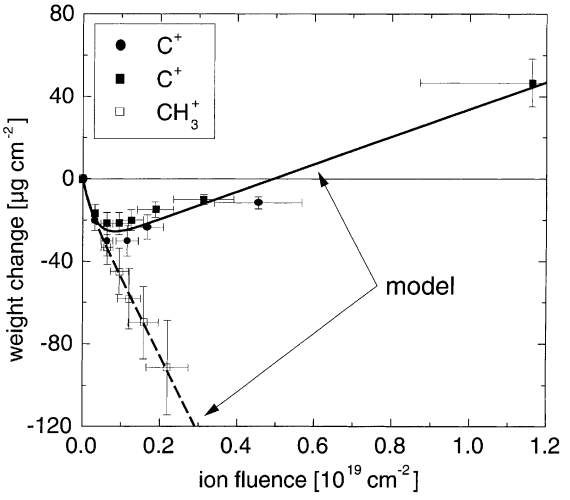

Fig. 3. Weight change of tungsten targets at 500°C as a function of irradiation fluence. For C^+, the experiments were performed on two targets denoted by circles and squares. The weight change according to the analytical model with parameters fitted to the experimental results is shown as in Fig. 2.

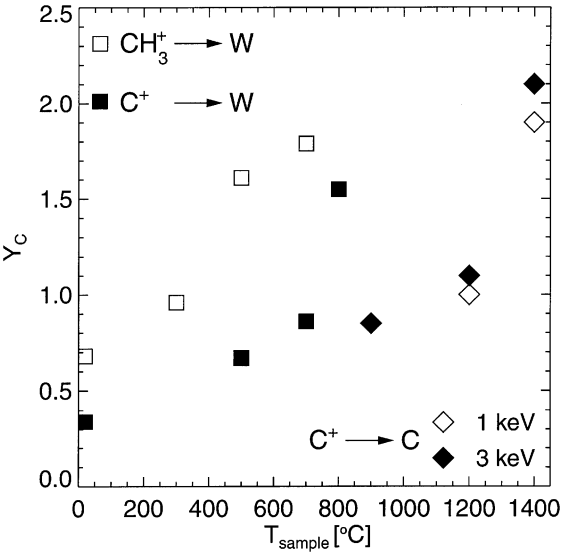

Fig. 4. Erosion yields as a function of target temperature. In addition results are shown for carbon self-sputtering yields [8].

would necessarily reduce the carbon erosion yield in the model to a value below 1.

Fig. 4 shows the erosion yields as a function of target temperature for both impacting species. All the values above 1 reflect cases where the initial weight loss continued up to the highest experimental fluence. Even taking into account the corresponding uncertainties, there is a clear increase of the obtained carbon erosion with increasing temperature. In addition, the values for CH_3^+ clearly exceed the yields for pure carbon bombardment. As discussed above, the respective differences cannot be explained by the additional carbon erosion of the impacting hydrogen ions. The steep increase of the erosion yield, above temperatures of ≈ 600°C to values exceeding measured carbon self-sputtering yields [8] (see Fig. 4), indicates that additional processes must be invoked to explain the experimental results. Apart from thermally enhanced erosion, a mechanism similar to radiation enhanced sputtering, diffusion processes might lead to an additional loss term of carbon from the target surface into the bulk [9]. With such an additional loss term, a correspondingly lower erosion yield would be required to model the observed weight change.

4.2. Total carbon deposition

The final amount of carbon deposited on the tungsten targets, as obtained from ion beam analysis after beam exposure, is shown in Fig. 5 for the different target temperatures. Since the final irradiation fluence varied from target to target, there is no systematic dependence on temperature. It is more important, however, to compare these measurements with the respective analytical model results, which were obtained using the erosion yield and scaling fluence from the fits to the weight change measurements. Except for one sample the

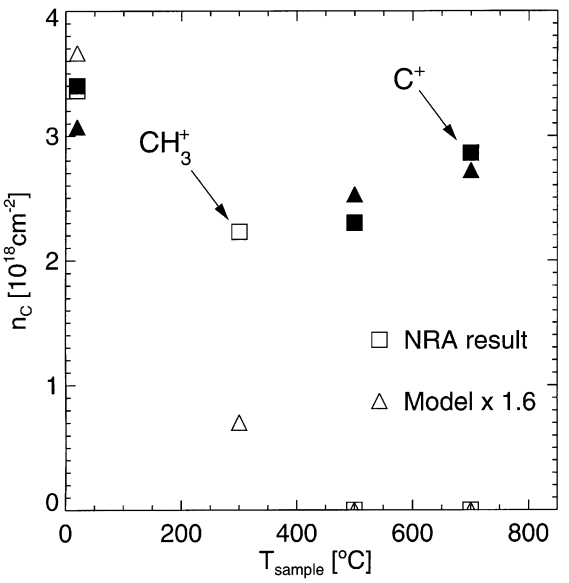

Fig. 5. Total amount of deposited carbon at the end of the irradiation measured by ion beam analysis. The corresponding amount derived from the model by using the parameters from the fit to the weight loss results is multiplied by a constant factor of 1.6 to account for systematic errors in the calibration of the ion beam current integration.

results agree very well with the experimental findings. The good agreement of the model with two independent measurements, i.e., weight loss and carbon deposition, is a good confirmation for the validity of the model assumptions.

5. Conclusions

Tungsten targets were irradiated with CH_3^+ radicals and carbon ions at different target temperatures. The measured weight change, as well as the final amount of carbon deposited on the targets, can be successfully described by a simple model. The model approximates the complicated implantation and erosion processes by a set of rate equations for the balance between erosion and deposition in an interaction layer of constant thickness.

The carbon erosion yields, obtained by fitting the model weight loss function to the experimental results, increase with target temperature. For target temperatures above ≈ 600°C, the results indicate a transition from net deposition to net erosion conditions. Thermally enhanced erosion and diffusion processes possibly could account for the increase of the carbon erosion yield at these temperatures.

The erosion yields, in the case of CH_3^+ bombardment, exceed the corresponding results for pure carbon bombardment by an amount, which cannot be explained by superposition of carbon self-sputtering and the additional erosion due to hydrogen impact.

References

[1] K. Krieger, H. Maier, R. Neu et al., J. Nucl. Mater. 266–269 (1999) 207.
[2] W. Eckstein, K. Krieger, J. Roth, J. Nucl. Mater. 258–263 (1998) 912.
[3] W. Eckstein, V.I. Shulga, J. Roth, Nucl. Instrum. and Meth. B 153 (1999) 415.
[4] D. Naujoks, W. Eckstein, J. Nucl. Mater. 220–222 (1995) 993.
[5] D. Naujoks, W. Eckstein, J. Nucl. Mater. 230 (1996) 93.
[6] E.W. Thomas, R.K. Janev, J. Smith, Nucl. Instrum. and Meth. B 69 (1992) 427.
[7] W. Eckstein et al., Sputtering Data, IPP Report IPP9/82, Garching, 1993, p.116ff.
[8] J. Roth, J. Bohdansky, W. Ottenberger, J. Nucl. Mater. 165 (1989) 193.
[9] K. Schmidt, J. Roth, W. Eckstein, Influence of diffusion on W sputtering by carbon, J. Nucl. Mater., this conference.